

## Article

# Study on SiO<sub>2</sub> Nanofluid Alternating CO<sub>2</sub> Enhanced Oil Recovery in Low-Permeability Sandstone Reservoirs

Jiani Hu <sup>1</sup>, Meilong Fu <sup>1,\*</sup>, Minxuan Li <sup>2</sup>, Honglin He <sup>3</sup>, Baofeng Hou <sup>1</sup>, Lifeng Chen <sup>1</sup> and Wenbo Liu <sup>1</sup>

<sup>1</sup> Hubei Key Laboratory of Oil and Gas Drilling and Production Engineering, College of Petroleum Engineering, Yangtze University, Wuhan 430100, China; hujiani0125@163.com (J.H.)

<sup>2</sup> CNOOC China Limited Hainan Branch, Haikou 570100, China

<sup>3</sup> Drilling and Production Technology Research Institute, PetroChina Qinghai Oilfield Company, Jiuquan 736202, China

\* Correspondence: fmlytze@163.com

**Abstract:** Water alternating gas (WAG) flooding is a widely employed enhanced oil recovery method in various reservoirs worldwide. In this research, we will employ SiO<sub>2</sub> nanofluid alternating with the CO<sub>2</sub> injection method as a replacement for the conventional WAG process in oil flooding experiments. The conventional WAG method suffers from limitations in certain industrial applications, such as extended cycle times, susceptibility to water condensation and agglomeration, and ineffectiveness in low-permeability oil reservoirs, thus impeding the oil recovery factor. In order to solve these problems, this study introduces SiO<sub>2</sub> nanofluid as a substitute medium and proposes a SiO<sub>2</sub> nanofluid alternate CO<sub>2</sub> flooding method to enhance oil recovery. Through the microcharacterization of SiO<sub>2</sub> nanofluids, comprehensive evaluations of particle size, dispersibility, and emulsification performance were conducted. The experimental results revealed that both SiO<sub>2</sub>-I and SiO<sub>2</sub>-II nanoparticles exhibited uniform spherical morphology, with particle sizes measuring 10–20 nm and 50–60 nm, respectively. The SiO<sub>2</sub> nanofluid formulations demonstrated excellent stability and emulsification properties, highlighting their potential utility in petroleum-related applications. Compared with other conventional oil flooding methods, the nanofluid alternating CO<sub>2</sub> flooding effect is better, and the oil flooding effect of smaller nanoparticles is the best. Nanofluids exhibit wetting modification effects on sandstone surfaces, transforming their surface wettability from oil-wet to water-wet. This alteration reduces adhesion forces and enhances oil mobility, thereby facilitating improved fluid flow in the rock matrix. In the oil flooding experiments with different slug sizes, smaller gas and water slug sizes can delay the breakthrough time of nanofluids and CO<sub>2</sub>, thereby enhancing the effectiveness of nanofluid alternate CO<sub>2</sub> flooding for EOR. Among them, a slug size of 0.1 PV approaches optimal performance, and further reducing the slug size has limited impact on improving the development efficiency. In oil flooding experiments with different slug ratios, the optimal slug ratio is found to be 1:1. Additionally, in oil flooding experiments using rock cores with varying permeability, lower permeability rock cores demonstrate higher oil recovery rates.

**Keywords:** SiO<sub>2</sub> nanofluid alternating CO<sub>2</sub>; microcharacterization; oil flooding experiment



**Citation:** Hu, J.; Fu, M.; Li, M.; He, H.; Hou, B.; Chen, L.; Liu, W. Study on SiO<sub>2</sub> Nanofluid Alternating CO<sub>2</sub> Enhanced Oil Recovery in Low-Permeability Sandstone Reservoirs. *Processes* **2023**, *11*, 2758. <https://doi.org/10.3390/pr11092758>

Academic Editors: Qingbang Meng, Bin Liang and Zhan Meng

Received: 3 August 2023

Revised: 8 September 2023

Accepted: 12 September 2023

Published: 15 September 2023



**Copyright:** © 2023 by the authors. Licensee MDPI, Basel, Switzerland. This article is an open access article distributed under the terms and conditions of the Creative Commons Attribution (CC BY) license (<https://creativecommons.org/licenses/by/4.0/>).

## 1. Introduction

The globally proven petroleum reserves are estimated to be an astonishing 1.2 trillion barrels. Despite primary and secondary oil recovery methods applied to the discovered reservoirs, approximately 377 million barrels of oil still remain trapped in porous media. Despite employing advanced technologies, fully exploiting these remaining reserves remains a challenging task. Therefore, more efficient and innovative enhanced oil recovery (EOR) techniques are required to extract these valuable resources [1,2]. According to the current statistical results, sandstone reservoirs account for about 70% of the low-permeability reservoirs in my country, which are characterized by poor physical properties, serious

heterogeneity, and fine pore throats. There are problems of high water injection pressure, the rapid rise of water cut, and low oil recovery rates in the production [3]. Many abandoned oilfields still contain residual oil saturation exceeding 30%. Moreover, in the later stages of water flooding development, water channeling and water flooding are severe, leading to low injection efficiency. While polymer flooding can effectively increase the recovery rate in medium to high-permeability formations, its direct application to low-permeability formations is hindered by high injection pressures. Therefore, technologies to enhance the recovery rate in low-permeability oil reservoirs still require urgent research and development [4–6].

Effectively developing residual oil resources has become a prominent topic in the petroleum industry, with tertiary oil recovery aimed at achieving oil recovery rates higher than the secondary baseline [7]. CO<sub>2</sub> flooding technology is a method used to enhance oil recovery by injecting liquid CO<sub>2</sub> into underground oil reservoirs. Upon injection, CO<sub>2</sub> dissolves in the oil, reducing its viscosity and facilitating its flow through the reservoir towards production wells. Additionally, the interaction between oil and CO<sub>2</sub> alters the pressure distribution and material balance within the reservoir, resulting in the liberation of some trapped oil from the pore spaces. This flooding effect, in conjunction with the flow of CO<sub>2</sub>, drives the liberated oil towards production wells for subsequent recovery to the surface. However, conventional water flooding or gas flooding may result in unfavorable mobility ratios, leading to inefficient cycling such as water fingering and gas channeling. Therefore, the injection method of water alternating gas (WAG) has been developed as an alternative approach [8,9]. Since the 1990s, several Chinese oilfields have successfully used the WAG injection technique to enhance oil recovery rates, particularly in heavy oil reservoirs [10,11]. Researchers have been devoted to optimizing the WAG injection process by studying factors such as gas injection rate, water injection rate, gas composition, etc. Additionally, researchers have been exploring the use of different gases, such as nitrogen, flue gas, and methane, during the WAG injection process [12,13]. Some major oilfields in China, including the Daqing, Shengli, and Changqing oilfields, have already implemented the WAG technique [14–18]. The successful application of WAG in these areas has been summarized and reviewed by Skauge et al., who studied 59 regions that utilized WAG. The research findings indicate that in all regions employing water–gas alternating injection, the average recovery rate can be increased by 10% [19]. However, the WAG technique also has its drawbacks. Interaction between the injected fluids and the reservoir rocks may cause reservoir damage, and the alternating injection of two different fluids involves certain technical complexities. Additionally, water–gas alternating injection is influenced by factors such as reservoir permeability, fluid properties, and injection rates [20–22]. The use of nanoparticles to enhance oil recovery is considered an economically efficient and environmentally friendly approach [23–26]. With the continuous advancement of nanotechnology and nanomaterials, significant achievements have been made in incorporating nanomaterials into the petroleum industry [27–30]. Nanofluids, stable colloidal dispersions or micellar dispersions, have demonstrated promising results in oil and gas reservoirs by employing a capillary-driven mechanism to improve the recovery of hydrocarbons. Nanoparticle dispersions within the nanofluids utilize this mechanism to form self-assembling wedge-shaped films that come into contact with the discontinuous phase, efficiently separating reservoir fluids (oil, paraffin, water, and/or gas) from the reservoir matrix [31–34]. In the WAG process, the addition of nanoparticles to the aqueous phase is known as nanofluid alternating gas injection technology. It is applied in medium and strongly oil-wet reservoirs to displace remaining oil, offering an efficient and cost-effective EOR method by enhancing both microscopic and macroscopic sweep efficiencies. This EOR technique improves the overall oil recovery by efficiently displacing the remaining oil in the reservoir through a combination of enhanced microscopic flooding efficiency and improved macroscopic sweep efficiency [35–39]. Previous studies have revealed various mechanisms of nanofluid oil displacement, such as reduced interfacial tension (IFT) [40,41], wettability alteration [42–44], asphaltene stabilization [45,46], reduced crude oil viscos-

ity [47], formation of nano-emulsions [48,49], and pore channel blocking [50] (Figure 1). These findings have confirmed that the use of nanoscale particles in oil field EOR measures yields promising results [51–53]. Nanoparticles have a significant impact on the wettability changes of sandstone reservoir rocks. They are a very effective oil recovery method and are cheap and environmentally friendly. Ju and Fan [54] studied how hydrophilic nano-SiO<sub>2</sub> particles can make the surface of sandstone moist. Wettens changes from lipophilic to hydrophilic. Li and Ole [55] used 2D and 3D imaging technology to observe that hydrophilic nano-SiO<sub>2</sub> particles formed a thin water film on the rock surface, preventing the solid surface from being wetted by oil and turning the oil-wet sandstone into water-wet sandstone. Ogolo et al. [56] found in the enhanced oil recovery experiment that nano-SiO<sub>2</sub> used ethanol as a dispersant, which can reduce the interfacial tension between oil and water and change the wettability of sandstone and is suitable for water-wet sandstone reservoir type rocks.

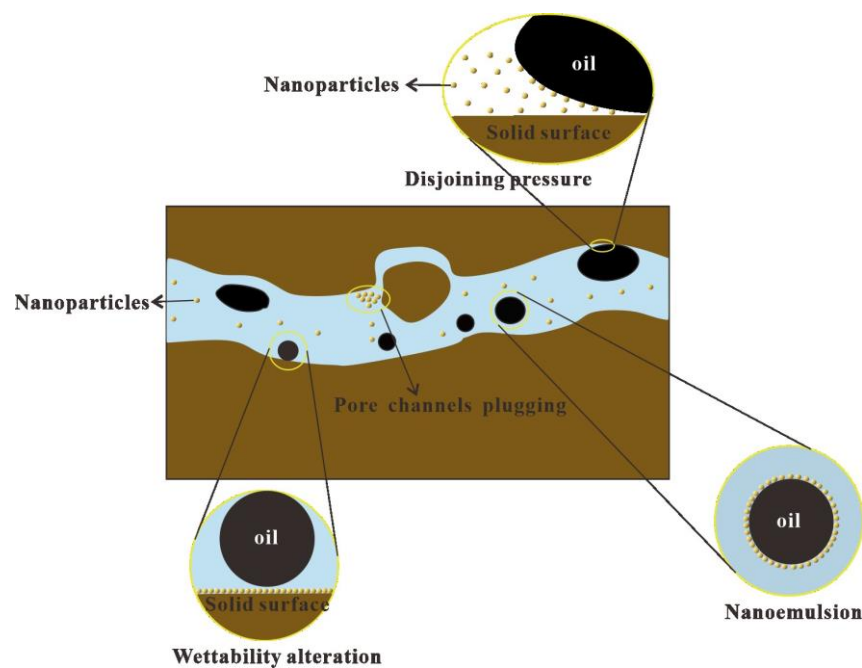


**Figure 1.** Oil displacement mechanism of nanofluids in porous media.

Al-Matroushi et al. [57] performed a simulation investigation of nanofluid alternating gas injection using the Eclipse-100 simulator. They conducted a 5 month injection of nanofluid into carbonate reservoirs, followed by 1 month CO<sub>2</sub> injection, employing a dual five-spot well pattern. The nanofluid alternating gas simulation results indicated a 13% increase in oil recovery compared to water–gas alternating injection. Moreover, the residual oil saturation experienced a reduction of 10%. Salem Ragab et al. [58] conducted a comparative study on the impact of two types of nanoparticles, Al<sub>2</sub>O<sub>3</sub> and SiO<sub>2</sub>, on interfacial tension. They observed a significant reduction in interfacial tension when adding Al<sub>2</sub>O<sub>3</sub> and SiO<sub>2</sub> nanoparticle solutions to salt solutions. Notably, the interfacial tension of the nanofluid containing SiO<sub>2</sub> was lower than that of the nanofluid containing Al<sub>2</sub>O<sub>3</sub>. Based on these findings, it was concluded that SiO<sub>2</sub> nanoparticles exhibit superior efficiency in enhancing oil recovery compared to Al<sub>2</sub>O<sub>3</sub> nanoparticles. Wang et al. [59] conducted experiments on artificial cores, simulating the geological conditions of a factory in the Daqing oilfield. These experiments involved water flooding followed by pressure reduction and nanosilica (SiO<sub>2</sub>) solution injection. The optimal injection volume of nanosilica solution under low-permeability conditions was determined. The results demonstrated that SiO<sub>2</sub> nanoparticles caused a wettability shift in the rock surface from hydrophilic to hydrophobic, leading to a further increase in oil recovery after water flooding. Amrouche et al. [60] investigated the impact of a magnetic field and alumina/iron oxide nanoparticles on oil-wet

carbonate reservoirs. The research findings demonstrated that this technology can lead to a cleaner and more efficient improvement in oil recovery from the Austin Chalk formation. Gallo and Erdmann [61] investigated nanofluid alternating gas injection using the CMG-GEM compositional simulator to study the consistency control mechanism. The study findings demonstrated that nanofluid alternating gas injection enhances carbon dioxide utilization and effectively controls the gas production rate, delaying gas breakthrough. Furthermore, this method improves volumetric sweep efficiency, resulting in higher and larger oil recovery rates. The research holds crucial implications for gas retention. Adel et al. [62] conducted multiple flooding experiments to study the impact of nanoparticle size on oil recovery rates, finding that using smaller-sized nanoparticles led to higher final oil recovery rates. This study bears important implications for gas retention. Mo et al. [63] observed that SiO<sub>2</sub>-stabilized CO<sub>2</sub> foam in sandstone cores can enhance oil recovery after water flooding. They also studied the influence of pressure, temperature, and rock properties on the CO<sub>2</sub> foam's capability to improve heavy oil recovery. The findings indicated that increasing pressure and decreasing temperature led to a higher recovery of residual oil during CO<sub>2</sub>/SiO<sub>2</sub> nanofluid flooding.

Previous research has demonstrated that nanofluid alternating gas injection is an effective method to enhance oil recovery. However, the mechanisms behind its enhanced recovery are not yet well understood. Most studies have focused on the role of nanoparticles, emphasizing their contribution to improved recovery rates. Nevertheless, the cooperative interactions between nanoparticles and CO<sub>2</sub> in porous media remain insufficiently explored. Therefore, there is a need to investigate the synergistic mechanisms of nanoparticles and CO<sub>2</sub> in porous media to fully understand their combined effects on enhanced recovery. Furthermore, research on the size and ratio of nanoparticle/CO<sub>2</sub> plugs and their impact on retarding water and gas breakthrough in different permeability reservoirs is limited. Comprehensive experimental studies are required to understand the effects and provide reliable strategies for reservoir development. Additionally, the applicability of nanoparticle alternating CO<sub>2</sub> injection in different permeability reservoirs needs further investigation.

The primary objective of this study is to employ a method involving SiO<sub>2</sub> nanofluid alternating CO<sub>2</sub> flooding, replacing traditional water–gas alternating processes for oil displacement experiments and conducting a performance assessment of this oil displacement system. SiO<sub>2</sub> particles were characterized through SEM analysis, infrared spectroscopy, particle size analysis, and dispersion experiments. The research includes evaluations of oil displacement effectiveness through experiments employing different injection methods, contact angle measurements, and viscosity testing before and after displacement. The study investigates the modification of rock surface wettability by SiO<sub>2</sub> nanoparticles in conjunction with CO<sub>2</sub>, elucidating the mechanism behind their synergistic action. By designing different nanofluid/CO<sub>2</sub> slug sizes and slug ratios, the study reveals their influence on delaying water and gas breakthrough times. Experimental investigations were conducted to assess the displacement effects of SiO<sub>2</sub> nanoparticle nanofluids alternated with CO<sub>2</sub> under various permeability conditions, and an in-depth examination of the mechanisms underlying enhanced oil recovery through SiO<sub>2</sub> nanofluid alternating CO<sub>2</sub> flooding was performed.

## 2. Materials and Methods

### 2.1. Materials and Instruments

The flooding setup for long cores is shown in Figure 2. The system includes a 50 cm long core holder, a thermostatic chamber, a pressure gauge, an ISCO high-pressure constant-rate flooding pump, a back-pressure valve, a data acquisition system, a gas flow meter, and an intermediate container, among others.

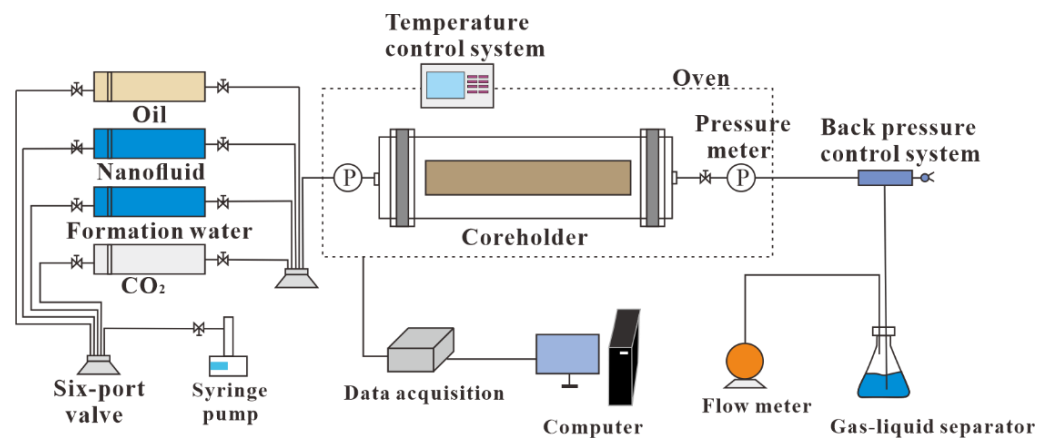


**Figure 2.** Core flooding experiment diagram.

Laboratory-made artificial sandstone cores (Figure 3) were prepared by bonding quartz sand with varying ratios of binder. These cores were compressed using a hydraulic press, and different permeabilities were achieved by controlling the binder/sand ratio and pressure. The experimental crude oil was a simulated oil formed by blending X oilfield dehydrated crude oil with kerosene (density  $0.826 \text{ g/cm}^3$ , viscosity at  $25 \text{ }^\circ\text{C}$  is  $43.37 \text{ mPa}\cdot\text{s}$ , Molecular Weight  $93.18 \text{ g/mol}$ ).  $\text{SiO}_2\text{-I}$  and  $\text{SiO}_2\text{-II}$  nanoparticles were provided by Degussa AG, Germany. Deionized water with a purity of 99.99% was prepared in the laboratory.  $\text{CO}_2$  gas with a purity of 99.99% was supplied by Wuhan Xinxing Gas Cylinder Co., Ltd. (Wuhan, China). For saturated core conditions, synthesized brine with a mineral content of  $30,466.93 \text{ mg/L}$  was utilized. The ionic element composition of the synthesized brine and core-related physical parameters are presented in Tables 1 and 2, respectively.

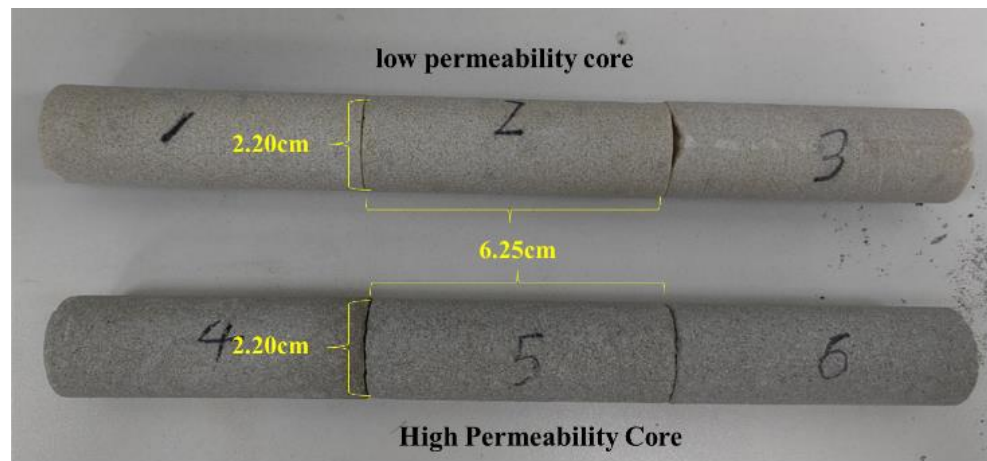


**Figure 3.** Physical map of rock cores.

**Table 1.** Ionic element composition of the synthesized brine.

Ion	Concentration, mg/L
$\text{Na}^+$	9625.19
$\text{Ca}^{2+}$	380.03
$\text{Mg}^{2+}$	1300.33
$\text{Cl}^-$	16,000.42
$\text{SO}_4^{2-}$	3000.50
$\text{HCO}_3^-$	160.46
Total	30,466.93

**Table 2.** Relevant physical properties of artificial cores.

Number	Length /cm	Diameter /cm	Permeability /mD	Porosity /%	Average Permeability /mD	Average Porosity/%
1	6.25	2.20	2.58	33.15		
2	6.25	2.20	2.34	34.28	2.49	33.05
3	6.25	2.20	2.56	31.71		
4	6.25	2.20	185.65	31.85		
5	6.25	2.20	206.43	32.37	196.88	31.57
6	6.25	2.20	198.55	30.48		

## 2.2. Experimental Methods

### 2.2.1. Characterization of Nanoparticles

SiO<sub>2</sub> powder was analyzed using a Thermo Fisher Scientific Inc. Nicolet 380 scanning electron microscope (Waltham, MA, USA). The SiO<sub>2</sub> powder was evenly spread on a conductive adhesive and fixed on a metal disc for sputter coating to enhance its conductivity. The coated sample was placed on the observation stage for morphology observation.

### 2.2.2. Zeta Potential Analysis

The Zeta potential analysis of the nano-SiO<sub>2</sub> was carried out by Malvern Panaco Instruments Ltd. Nano ZS90 laser particle size distribution analyzer (Malvern, UK). At room temperature, nanofluids of different concentrations were sonication dispersed for 30 min, and then the dispersion system was taken out and poured into the sample pool. During the experiment, the sample cell was first set to 45 °C, each sample was measured at least 5 times, the data with large errors were eliminated, and the average value was taken.

### 2.2.3. Particle Size Test

The SiO<sub>2</sub> nano-dispersion liquid with a mass fraction of 0.15% was prepared, and the particle size distribution of the SiO<sub>2</sub> nano-fluid was analyzed and determined by the Nanbrook Omni laser particle size distribution analyzer (New York, NY, USA) of Brookhaven Instrument Company.

### 2.2.4. Emulsifying Properties

At 45 °C, a mixture of oil and water in a volume ratio of 3:7 was added to a test tube. The mixture was homogenized using an IKA T18B homogenizer at 2000 r/min and then placed in a thermostatic chamber. After 30 min of static settling, the test tube was shaken 120 times, followed by immediate placement on a test tube rack in a 45 °C thermostatic chamber. The volume of separated water phase in the test tube was recorded within 2 h, and the water separation rate  $\delta$  was calculated according to Formula (1). The microstructure, particle size, and distribution of the emulsion after 2 h of static settling were observed using an Enoptik Ltd. Axbstar Plus fluorescence microscope (Jena, Germany).

$$\delta = \frac{V_1}{V_2} \times 100\% \quad (1)$$

In the formula,  $\delta$  represents the water separation rate, expressed in percentage, %;  $V_1$  stands for the volume of water separated from the emulsion, measured in milliliters, mL;  $V_2$  refers to the total volume of water in the emulsion, also measured in milliliters, mL.

### 2.2.5. Contact Angle Test

Using the Kruss Ltd. DSA25 automatic contact angle goniometer (Hamburg, Germany), the effect of nanofluids on the wettability of solid surfaces in the petroleum field was investigated. Glass slides were immersed in n-heptane/crude oil for one week, followed by cleaning with n-heptane until colorless, and then allowed to dry for 1–2 days. Afterward,

the glass slides were separately immersed in two types of nanofluids for two days. A water droplet was injected onto the glass slide surface using a syringe, and the glass slide was adjusted to a horizontal position. The contact angle of the water droplet on the glass slide surface was measured using the contact angle goniometer, and images of the contact angle were captured and saved.

### 2.2.6. Core Flooding Experiment

Through core flooding experiments, a systematic study was conducted to investigate the effect and oil flooding mechanism of SiO<sub>2</sub> nanofluid alternating CO<sub>2</sub> on EOR in reservoir cores. A comparative analysis was performed to explore the feasibility of the SiO<sub>2</sub> nanofluid alternating CO<sub>2</sub> flooding method for improving heavy oil recovery. The research focused on different injection methods, different gas–water slug ratios, different slug sizes, and the impact of different permeability cores on the oil flooding efficiency. The objective was to determine the optimal injection parameters for SiO<sub>2</sub> nanofluid alternating CO<sub>2</sub> flooding in the context of EOR in petroleum reservoirs.

## 3. Results and Discussion

### 3.1. Performance Measurements

SEM images of SiO<sub>2</sub>-I and SiO<sub>2</sub>-II nano powders are shown in Figure 4, revealing two distinct sizes of 10–20 nm and 50–60 nm, respectively. Both types exhibit uniform spherical shapes with well-dispersed and evenly sized particles. The dispersion solution was prepared with a concentration of 0.15 wt% for SiO<sub>2</sub>-I and SiO<sub>2</sub>-II nanoparticles, and the particle size measurement is shown in Figure 5, indicating particle sizes of 115 nm for SiO<sub>2</sub>-I nanoparticles in water and 207 nm for SiO<sub>2</sub>-II.

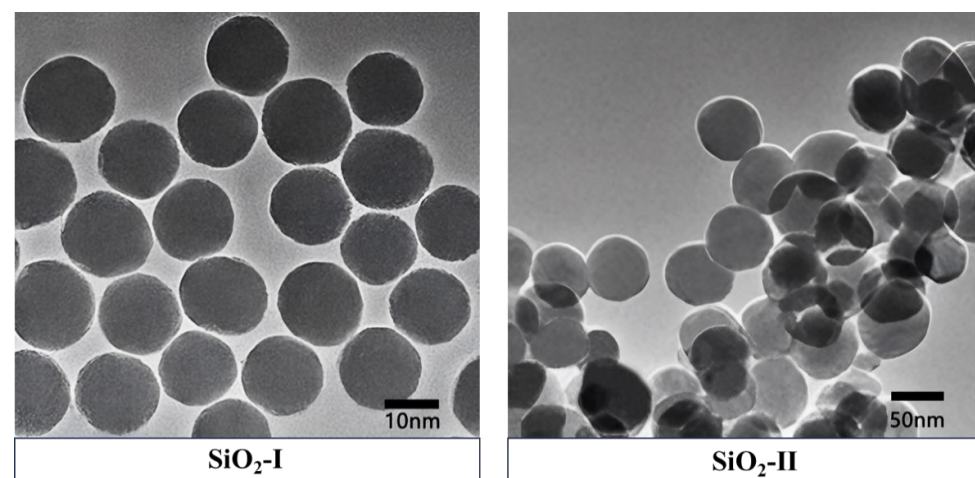


Figure 4. SEM images of nano powders.

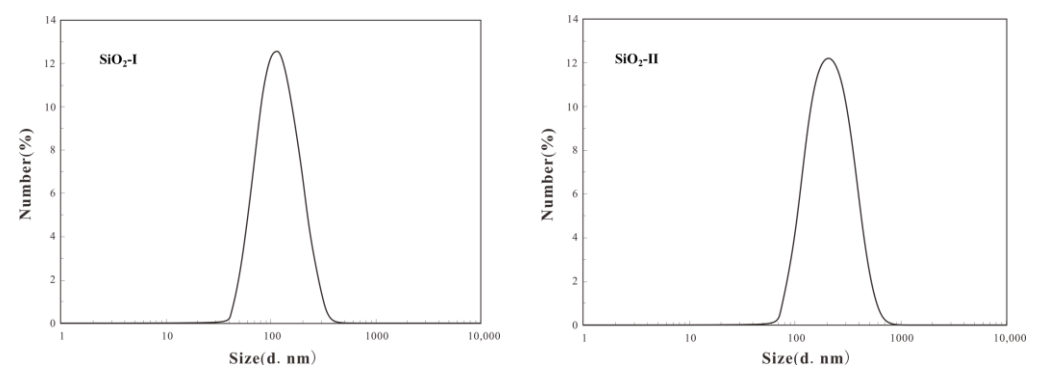


Figure 5. The particle size of nanoparticles in aqueous solution.

Prior to injecting the nanofluids into the rock core samples, the stability of 0.15 wt% concentration of SiO<sub>2</sub>-I and SiO<sub>2</sub>-II dispersion solutions was observed for a period of 7 days, as shown in Figure 6. No precipitation was observed at the bottom of the solution. Figure 7 shows the Zeta potential data for silica. It can be seen from the figure that the Zeta potentials of the two SiO<sub>2</sub> particles are both negative. This is because silicon dioxide in the sample solution is a non-metallic oxide, and its particles are dispersed in water to absorb negatively charged particles. It is generally believed that the greater the absolute value of the Zeta potential, the better the stability of the solution. The absolute values of the Zeta potentials of SiO<sub>2</sub>-I and SiO<sub>2</sub>-II nanofluids are both above 30 mV, and the absolute values of the Zeta potentials of SiO<sub>2</sub>-I are larger than SiO<sub>2</sub>-II as a whole. When the concentration is 0.15%, the negative value is  $-39.7$  mV, so it is considered that the dispersion stability of SiO<sub>2</sub>-I-I is better.

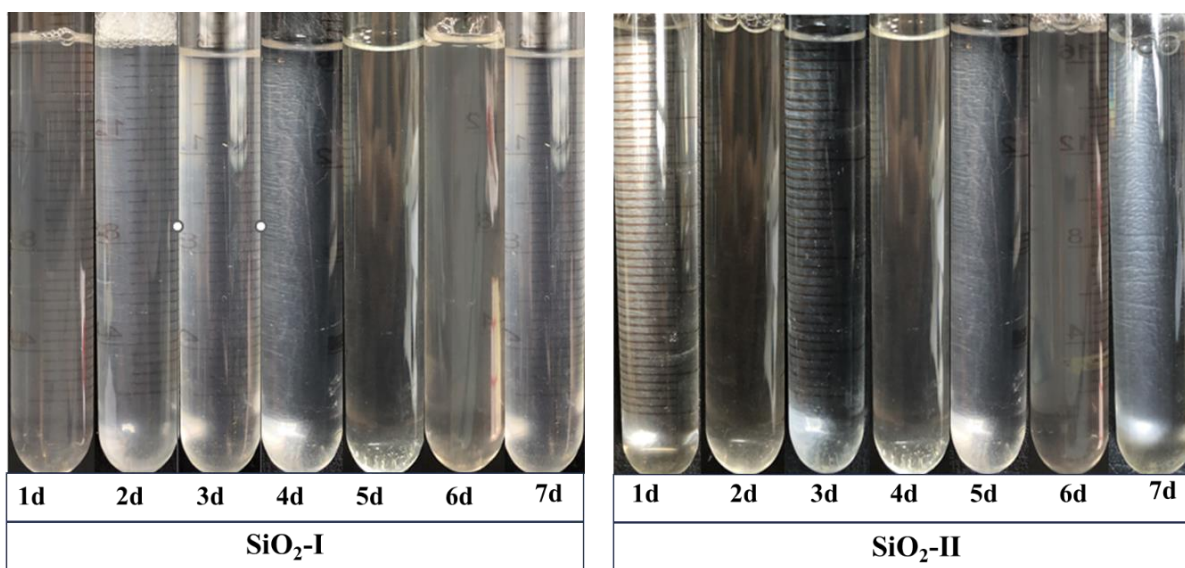


Figure 6. Nano-dispersion solution 7 day variation chart.

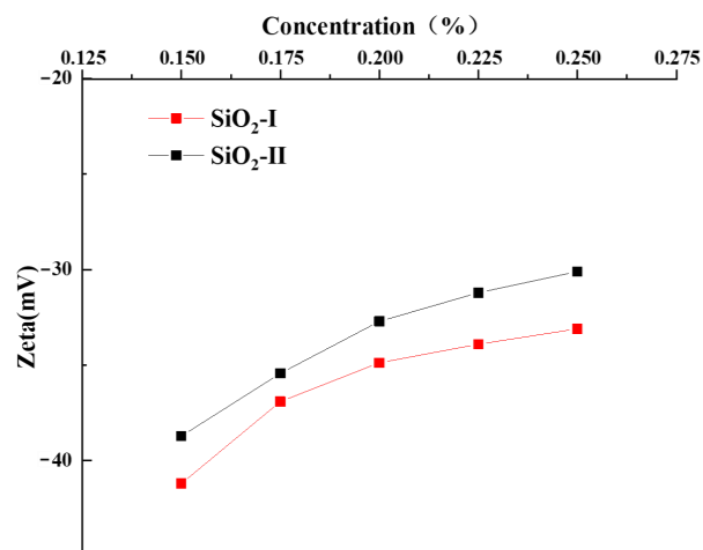


Figure 7. Effect of concentration on Zeta potential.

From the FTIR of SiO<sub>2</sub> (Figure 8), it can be observed that there are typical stretching vibration absorption peaks of Si–O–Si at  $476\text{ cm}^{-1}$ ,  $803\text{ cm}^{-1}$ , and  $1093\text{ cm}^{-1}$ . There is a stretching vibration absorption peak of Si–OH at  $969\text{ cm}^{-1}$ , and at  $3431\text{ cm}^{-1}$ , there is a stretching vibration absorption peak of –OH. The absorption peak at  $1634\text{ cm}^{-1}$  in the

H–O–H bending vibration is due to the presence of residual moisture adsorbed on the nano  $\text{SiO}_2$ , and the condensation between hydroxyl groups leads to the aggregation of nano  $\text{SiO}_2$  particles forming Si–O–Si bonds.

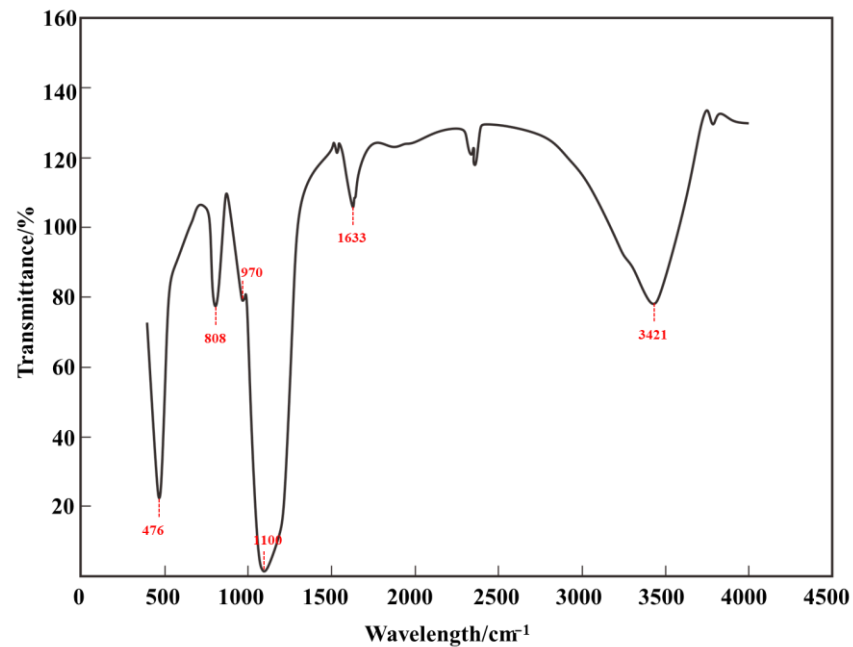


Figure 8. FTIR of  $\text{SiO}_2$ .

Using 0.15 wt%  $\text{SiO}_2$ -I and  $\text{SiO}_2$ -II nanofluids, an oil-in-water emulsion was prepared with an oil-to-water ratio of 3:7 and allowed to stand at 45 °C for 2 h. The physical appearance of the emulsion before and after emulsification is shown in Figure 9, with the final water cut stabilizing at around 60%, demonstrating good stability. The emulsion's microstructure and particle size distribution were observed using a biological fluorescence microscope, as shown in Figure 10. The emulsion primarily exhibited a morphology of large droplets, densely packed and with small droplets as the main constituents. There were also a few larger droplets with sizes between 1~10  $\mu\text{m}$ . Of great significance, these droplets adhered to each other, showing that nanoparticles are not prone to agglomeration.

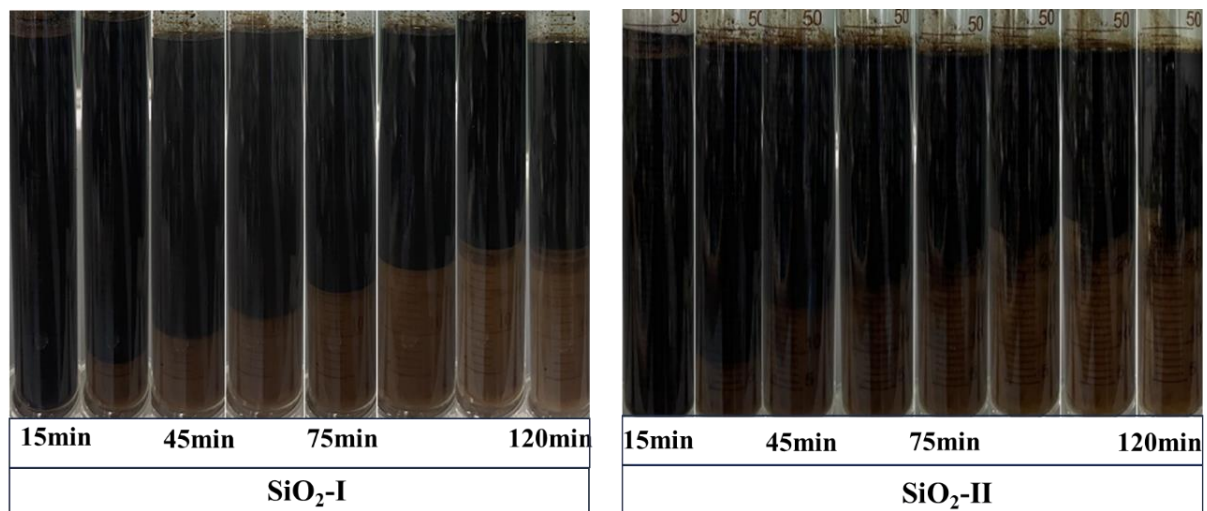


Figure 9. Dynamic water separation process of the emulsion at 120 min.

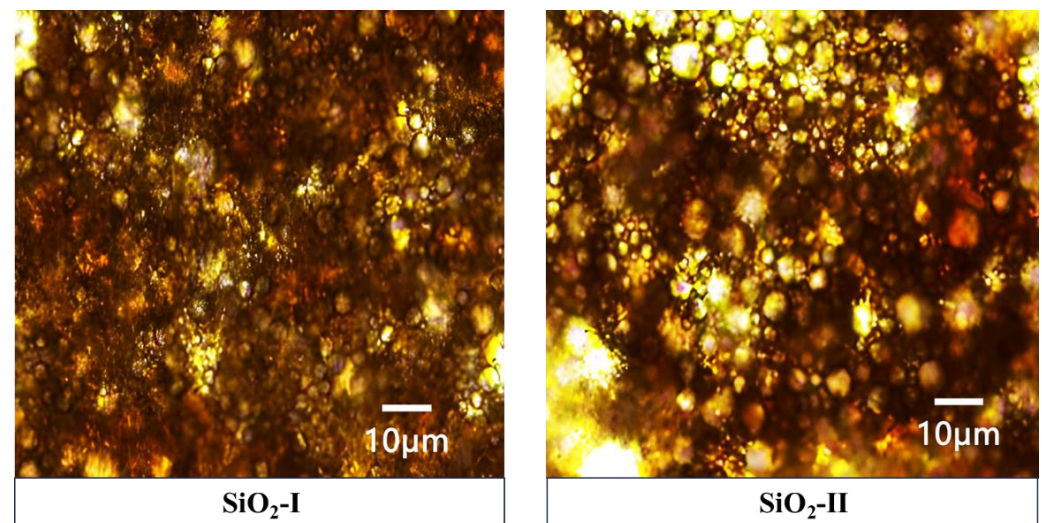


Figure 10. Microscopic morphology of the emulsion.

### 3.2. Oil Flooding Tests

#### 3.2.1. Different Injection Methods

At a constant experimental temperature of 45 °C, an initial injection pressure of 6.5 MPa, a water/nanofluid injection rate of 0.15 mL/min with each circulation injecting 0.2 PV, and a CO<sub>2</sub> injection rate of 0.25 mL/min with each circulation injecting 0.1 PV, low-permeability cores were employed to investigate different injection systems (water, CO<sub>2</sub>, WAG, and nanofluid alternating CO<sub>2</sub> flooding). The recovery efficiencies were compared, and the relationship between the oil recovery factor and injected pore volume is depicted in Figure 11.

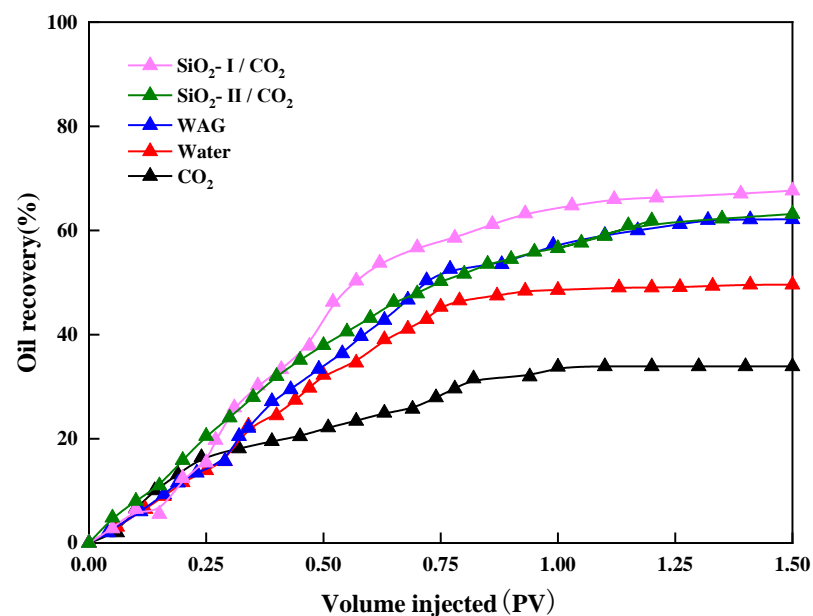


Figure 11. Comparison of the oil recovery factor and injected pore volume under different injection methods.

From Figure 11, it is evident that among the four different oil flooding schemes, SiO<sub>2</sub>-I and SiO<sub>2</sub>-II alternating CO<sub>2</sub> flooding exhibit higher recovery efficiencies compared to other flooding methods. Among them, SiO<sub>2</sub>-I alternating CO<sub>2</sub> flooding achieves the highest oil recovery factor, reaching up to 67.65%, while pure CO<sub>2</sub> flooding exhibits the lowest oil recovery factor. This can be attributed to the experimental injection pressure being

below the minimum miscibility pressure (MMP) of CO<sub>2</sub> and oil, resulting in limited phase mixing between oil and gas, and consequently leading to a lower oil recovery factor in pure CO<sub>2</sub> flooding.

In the process of nanofluid flooding, changes in wettability also significantly impact reservoir characteristics, such as relative permeability characteristics, the distribution of fluids (hydrocarbon and aqueous phases) in the pore network, and fluid flow during recovery. Alterations in wettability play a crucial role in the mechanisms of nanofluid oil flooding [64,65]. To investigate the wettability of reservoir rocks, we conducted contact angle measurements, which is one of the most common methods for assessing surface wettability. The contact angle is a physical quantity that measures the degree of liquid spreading on a solid surface. By measuring the contact angle between a liquid droplet and the rock surface, we can understand the interaction strength and changes in wettability between the liquid and the rock surface. For the investigation of the wettability of the surface layer of the rock, a small piece of rock was cut to test the changes in contact angle before and after the flooding. The results are shown in Figure 12.

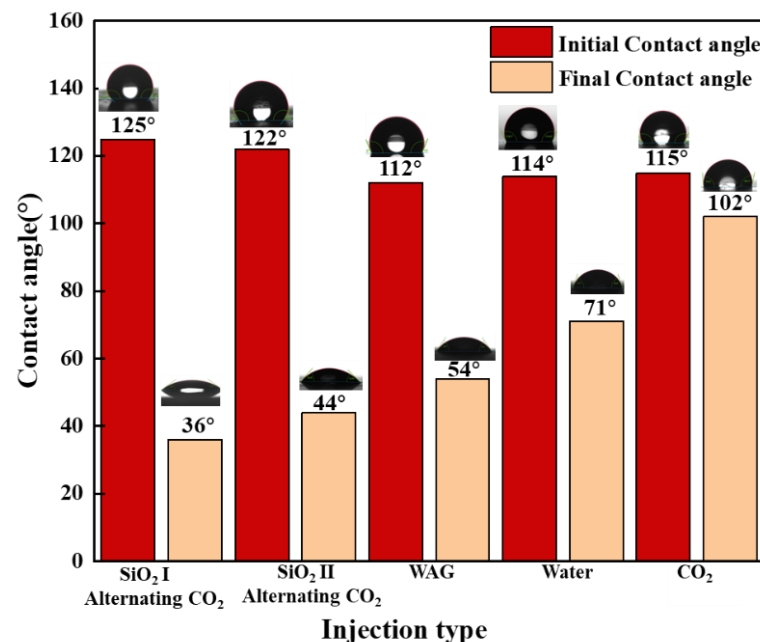


Figure 12. Contact angle of rocks before and after different injection methods.

From Figure 12, it is evident that the initial wettability of the oil-saturated core is strongly oil-wet. Among the different injection methods, Type I nanofluid alternating CO<sub>2</sub> flooding induces the most significant change in the core surface contact angle, shifting the wettability to strong hydrophilicity. As the particle size of the nanofluid displacement agent decreases, its specific surface area increases accordingly, leading to a higher concentration of effective molecules per unit volume. When the nanofluid displacement agent is injected into the rock, it interacts with the rock surface, forming a monomolecular thin film. This film alters the wettability characteristics of the rock surface, significantly reducing the adsorption force of the crude oil on the rock surface. This effect, in turn, promotes an increase in the crude oil recovery factor and lowers the water injection pressure. These findings contribute to the overall improvement in oil recovery.

The addition of nanoparticles can regulate the distribution of displacing fluid within the pores, preventing premature channel formation, thus enabling the displacing agent to be more uniformly dispersed within the rock. This ensures that the displacing agent not only flows through larger pores but is also evenly distributed within smaller pores, thereby avoiding bypassing the crude oil. This optimization of fluid distribution aids in ensuring that SiO<sub>2</sub> nanofluids are more fully in contact with crude oil, improving the flow

of crude oil in pores to effectively release the crude oil from the pores. In this experiment, nanoscale SiO<sub>2</sub> particles with a high surface area and excellent dispersion adhere to the rock surface, forming a coverage layer that modifies the chemical properties of the rock surface. As a result, the originally oil-wet surface becomes water-wet. The increased water-wetting promotes better contact between the water and the rock surface, resulting in a relatively reduced permeability of the wetting phase (water), while the permeability of the non-wetting phase (oil) increases as it no longer adheres to the rock surface. This weakening of oil-rock surface interactions reduces adhesion forces, thereby enhancing oil mobility.

The SiO<sub>2</sub> nanoparticles can form a substantial interfacial film at the oil-water interface, significantly enhancing the stability of the emulsion. This emulsifying effect disperses the oil within the aqueous phase, reducing its continuous presence within the rock pores. As a result, it lowers adhesion and oil viscosity, ultimately improving oil displacement efficiency. Table 3 presents the viscosity measurement results of oil displaced under different injection methods in low-permeability reservoirs. Among them, SiO<sub>2</sub>-I alternating CO<sub>2</sub> flooding shows the lowest viscosity of the displaced crude oil. When CO<sub>2</sub> dissolves in the crude oil, it causes oil expansion and reduces its viscosity. The dissolution of CO<sub>2</sub> in the crude oil leads to an increase in oil volume, thereby lowering the oil's adhesion to the rock pores, making it easier to displace the oil from the rock. Additionally, CO<sub>2</sub> dissolution enhances the fluidity of the crude oil, facilitating smoother flow within the pores.

**Table 3.** Viscosity measurement after different injection in the low-permeable core.

Low-Permeable Core Injection	Viscosity/mPa·s
Viscosity of crude oil in preliminary test	43.37
SiO <sub>2</sub> -I alternating CO <sub>2</sub>	35.21
SiO <sub>2</sub> -II alternating CO <sub>2</sub>	36.47
WAG	38.55
Water	43.28
CO <sub>2</sub>	38.83

This dissolution and expansion effect of CO<sub>2</sub> provides dynamic support for the displacement by nanoscale SiO<sub>2</sub> since it increases the fluidity of the oil, making it more amenable to nanoscale SiO<sub>2</sub> displacement. Overall, the nanoscale SiO<sub>2</sub> and CO<sub>2</sub> complement each other during the displacement process. The filling effect of nanoscale SiO<sub>2</sub> and the alteration of wettability compensate for CO<sub>2</sub>'s limitations in low-permeability rocks by improving the pore structure and reducing oil adhesion, making the oil flow more efficiently. Simultaneously, CO<sub>2</sub> dissolution, expansion, and displacement assist the nanoscale SiO<sub>2</sub> in displacing the reservoir, driving the oil forward. This mutual interplay creates a synergistic effect, significantly enhancing the efficiency of nano-fluid alternating CO<sub>2</sub> flooding, leading to a substantial increase in the recovery rate.

### 3.2.2. Different Slug Sizes

Using low-permeability rock cores, the impact of slug size on the efficacy of alternating nanofluid and CO<sub>2</sub> flooding in EOR was investigated. The experimental results depicted in Figure 13 indicate that the 0.05 PV per slug shows slightly higher oil recovery compared to the 0.1 PV per slug, while the 0.15 PV per slug exhibits the lowest oil recovery. Furthermore, the breakthrough time for both gas and water in the 0.05 PV per slug was delayed. Therefore, it can be inferred that smaller slug sizes are less susceptible to channeling, consequently leading to a further increase in oil recovery.

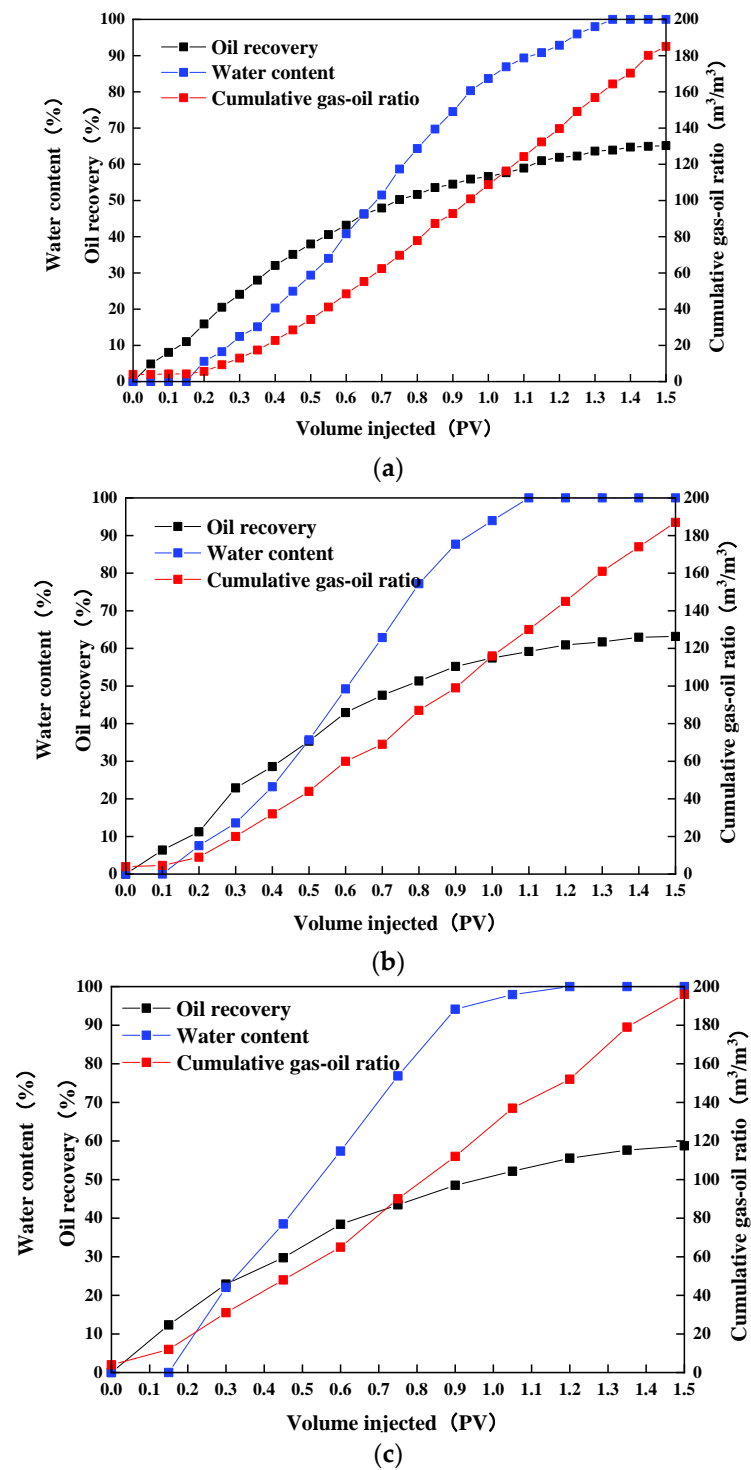


**Figure 13.** Impact of slug size on the efficacy of alternating nanofluid and CO<sub>2</sub> flooding in EOR. (a) 0.05 PV per slug. (b) 0.1 PV per slug. (c) 0.15 PV per slug.

The smaller gas and water slug volumes lead to a delay in the breakthrough time for nanofluid and CO<sub>2</sub> slug, thus improving the effectiveness of alternating nanofluid and CO<sub>2</sub> flooding. The oil recovery performance of the 0.05 PV and 0.1 PV slugs is comparable, with insignificant differences in the CO<sub>2</sub> storage capacity, suggesting that when gas and water slug volumes are small, the influence of slug size on the effectiveness of alternating nanofluid and CO<sub>2</sub> flooding is not significant. Therefore, it can be inferred that the slug size of 0.1 PV is close to optimal, and further reducing the slug size has limited impact on the improvement of reservoir development.

### 3.2.3. Different Slug Ratios

Low-permeability cores were utilized to investigate the impact of the nanofluid -CO<sub>2</sub> slug ratio on the development effectiveness of nanofluid alternating CO<sub>2</sub> flooding. In Figure 13, the nanofluid-CO<sub>2</sub> slug ratios are 1:1, 3:1, and 1:3, respectively. It is evident from Figure 14 that the nanofluid-CO<sub>2</sub> slug ratio of 1:1 exhibits the highest recovery rate, with the latest water breakthrough time. Hence, it is concluded that the most favorable development effect is achieved with a slug ratio of 1:1 in nanofluid alternating CO<sub>2</sub> flooding, while excessively large or small slug ratios may adversely affect the development process. The primary reason for this phenomenon is that excessively large or small slug ratios lead to the rapid breakthrough of nanofluid or CO<sub>2</sub> slugs, resulting in a swift increase in the water cut or production gas-oil ratio, thereby influencing the development effect of nanofluid alternating CO<sub>2</sub> flooding. In the nanofluid-CO<sub>2</sub> slug ratio of 3:1, the amount of CO<sub>2</sub> storage decreases as the water slug expands, displacing a portion of CO<sub>2</sub> gas during water flooding, leading to a reduction in CO<sub>2</sub> storage. Conversely, in the nanofluid-CO<sub>2</sub> slug ratio of 1:3, the gas slug increases, causing the gas flooding process to prolong and displacing a portion of water, resulting in the increased gas occupancy of the pore volume and subsequently increasing CO<sub>2</sub> storage.

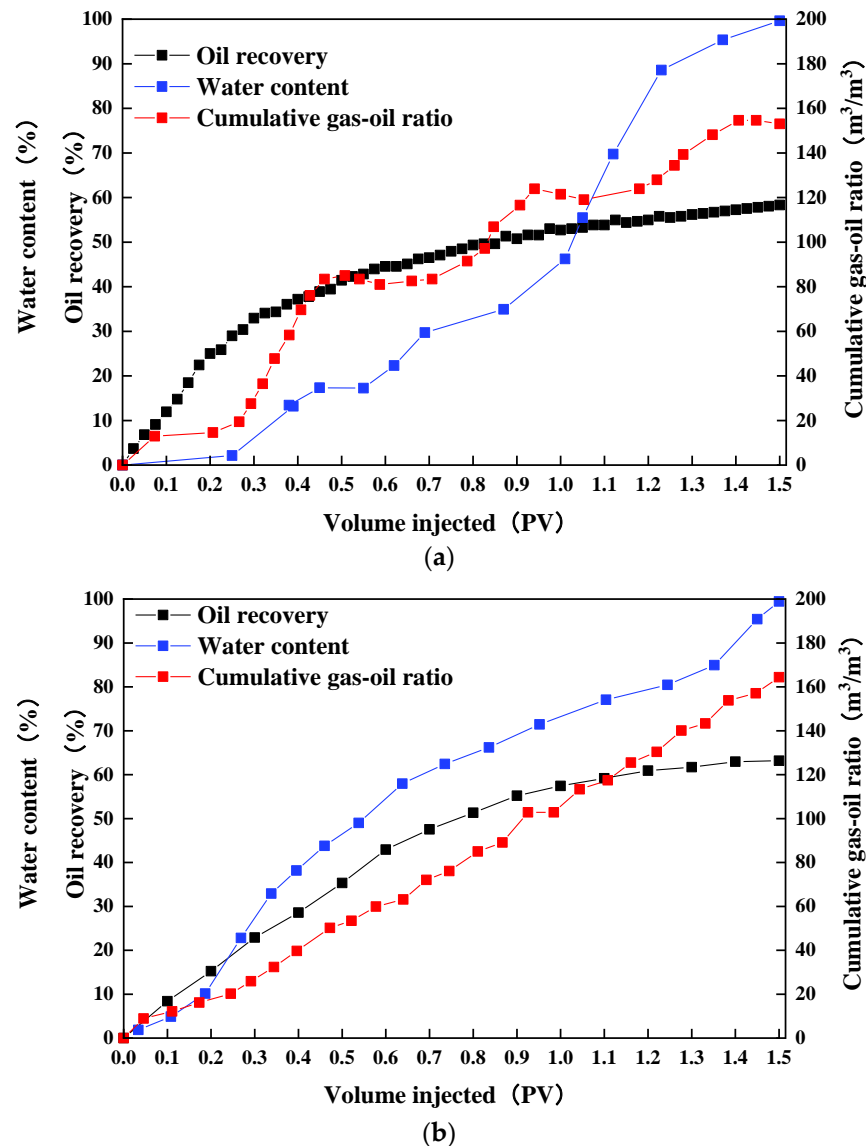


Figure 14. Cont.

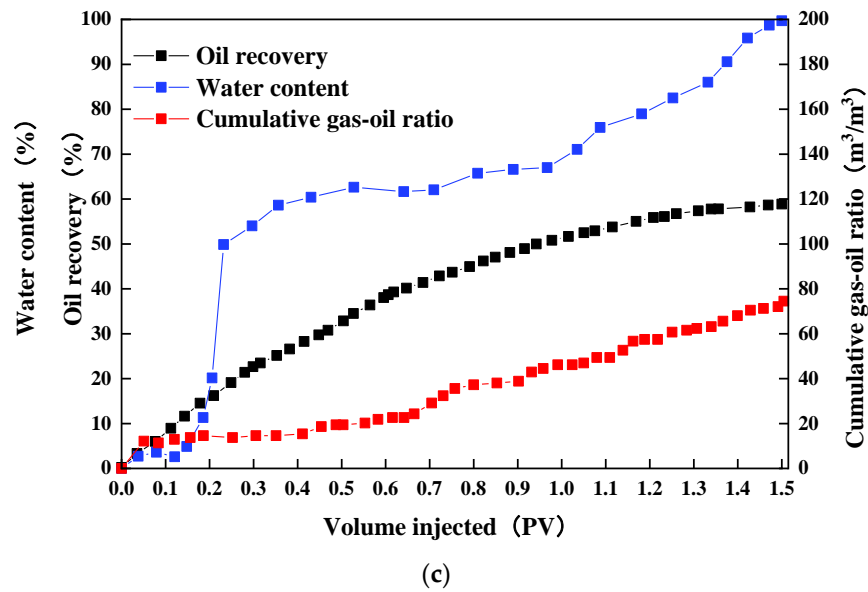


Figure 14. Impact of nanofluid–CO<sub>2</sub> slug ratio on the efficacy of flooding in EOR. (a) SiO<sub>2</sub>-I/CO<sub>2</sub> Slug ratio 1:3. (b) SiO<sub>2</sub>-I/CO<sub>2</sub> Slug ratio 1:1. (c) SiO<sub>2</sub>-I/CO<sub>2</sub> Slug ratio 3:1.

Therefore, an appropriate nanofluid–CO<sub>2</sub> slug ratio can effectively control the water cut, achieving the optimal balance between the filling effect and displacement effect, thereby significantly improving the oil recovery factor. It leverages the high efficiency of CO<sub>2</sub> in oil displacement while avoiding premature gas channeling, enhancing the CO<sub>2</sub> sweep efficiency and thus improving the oil recovery performance.

#### 3.2.4. Flooding in Cores with Different Permeabilities

To study the influence of various rock types on alternating nanofluid and CO<sub>2</sub> flooding for EOR, two distinct injection methods, namely water–gas alternating flooding and nanofluid alternating CO<sub>2</sub> flooding, were implemented on high and low-permeability rock cores. As illustrated in Figure 15, our experimental results indicate that, under the given conditions and using the chosen materials, alternating nanofluid and CO<sub>2</sub> flooding demonstrate superior oil recovery performance in low-permeability rock core samples.

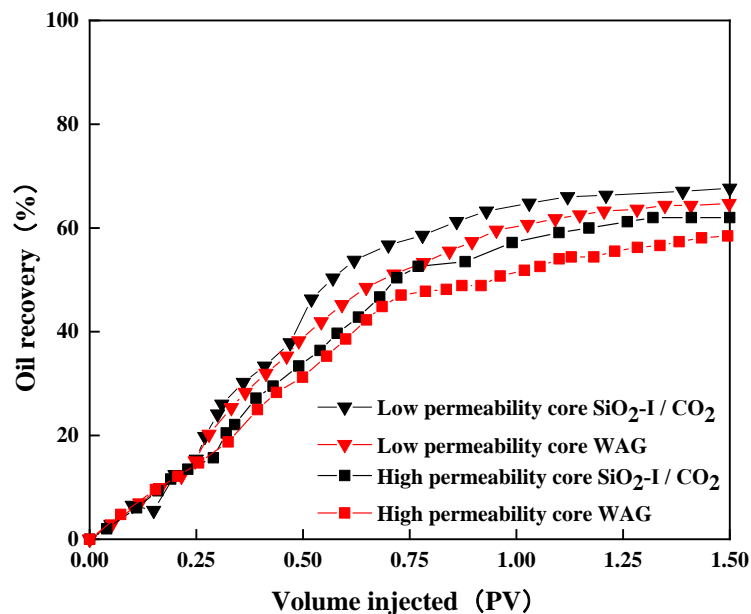
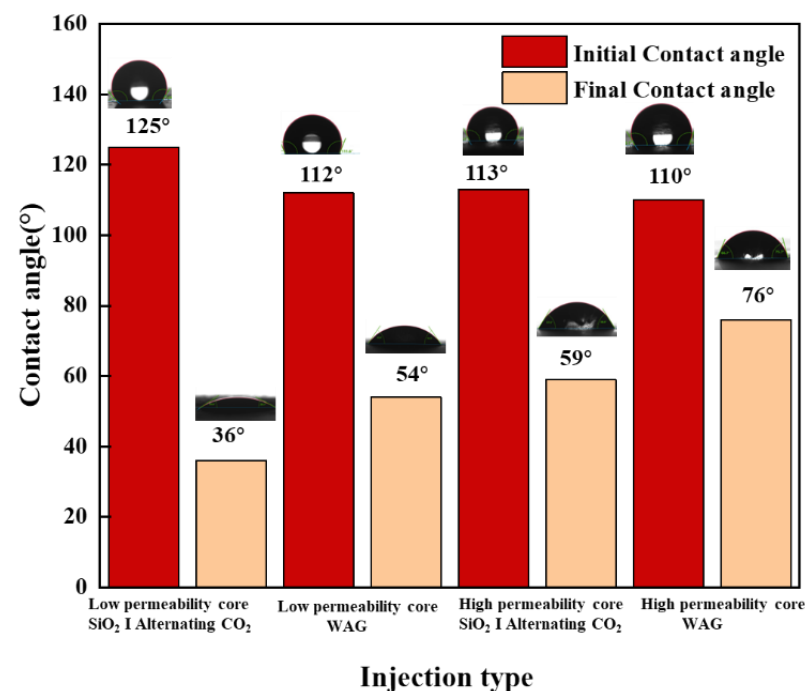


Figure 15. Oil recovery factor in different permeability rock cores.

Low-permeability rocks are characterized by their small pore sizes and low pore connectivity, leading to increased oil adsorption on the rock surface due to the larger surface area and smaller pore size. Consequently, a significant fraction of the oil gets trapped within the pores, resulting in poor oil flow and hindered oil recovery. The introduction of SiO<sub>2</sub> nanoparticles with smaller dimensions serves to occupy the micro-voids in the low-permeability rock pores, thereby improving pore connectivity and reducing pore channel blockages, ultimately enhancing oil flow mobility and increasing the oil recovery factor. Moreover, the surface of SiO<sub>2</sub> nanoparticles bears a negative charge, enabling them to adsorb and stabilize positively charged oil droplets. Within low-permeability rocks, the interactions between SiO<sub>2</sub> nanoparticles and oil droplets lead to a weakening of the adhesion forces between the oil and rock surface, thereby facilitating the detachment of oil droplets from the rock surface and, consequently, increasing the oil recovery factor.

The assessment of contact angles was conducted to examine alterations in wettability, as illustrated in Figure 16. The results of the contact angle measurements suggest a more pronounced improvement in wettability in low-permeability rock cores, with alternating nanofluid and CO<sub>2</sub> flooding exhibiting the most favorable performance. The reduced size of nanoparticles allows them to fill the microscopic voids in rock pores, leading to a reduction in pore volume and an increase in effective pore volume and permeability. This filling effect significantly contributes to improved displacement efficiency and facilitates the expulsion of oil from the rock matrix.



**Figure 16.** Contact angle of rocks before and after oil displacement in different permeability rock cores.

#### 4. Conclusions

This study investigates the mechanism by which alternating nanofluid and CO<sub>2</sub> flooding enhances oil recovery through research on nanofluid stability, nanofluid-induced wettability alteration on rock surfaces, and experimental studies on alternating nanofluid and CO<sub>2</sub> flooding. The final conclusions and findings are as follows:

1. Both SiO<sub>2</sub>-I and SiO<sub>2</sub>-II exhibit good sphericity and monodispersity, with excellent dispersion stability in the aqueous phase, and they demonstrate good emulsification properties with the oil phase.

2. Compared to other conventional oil displacement methods, the SiO<sub>2</sub>-I nanofluid alternating CO<sub>2</sub> flooding scheme shows the most favorable performance, achieving a recovery rate of up to 67.65%. Contact angle experiments reveal that SiO<sub>2</sub> nanoparticles have the capability to modify the wettability of hydrophilic solid surfaces, converting them into hydrophilic surfaces. During the oil displacement process, SiO<sub>2</sub> nanoparticles enhance pore connectivity and oil mobility in rock formations through pore-filling, wettability alteration, and emulsification, thereby increasing oil displacement efficiency. The viscosity of the displaced crude oil was found to be the lowest in the SiO<sub>2</sub>-I alternating CO<sub>2</sub> flooding scenario. The dissolution and expansion effects of CO<sub>2</sub> provided dynamic support for the displacement process with nanoscale SiO<sub>2</sub>, leading to a synergistic enhancement. This combination significantly improved the efficiency of nanofluid alternating CO<sub>2</sub> flooding and effectively increased the oil recovery rate in low-permeability reservoirs.
3. Smaller gas and water slugs lead to better performance in alternating nanofluid and CO<sub>2</sub> flooding. However, when the gas and water slugs are too small, their influence on the development effect of alternating nanofluid and CO<sub>2</sub> flooding becomes insignificant and may instead increase operational costs in field applications. Both excessive and inadequate gas–water slug ratios can adversely impact the development effect, primarily due to the rapid increase in the water cut or gas–oil ratio. The experimental study on the gas–water slug ratio reveals that the best development effect is achieved with a gas–water slug ratio of 1:1 in nanofluid alternating CO<sub>2</sub> flooding.
4. Alternating nanofluid and CO<sub>2</sub> flooding demonstrates a superior oil recovery factor in low-permeability rock formations. Low-permeability rock formations with small pores and poor pore connectivity allow smaller particles to facilitate more efficient transport through the porous media. SiO<sub>2</sub> nanoparticles can fill pores, enhance pore connectivity, reduce residual oil trapping, and increase oil mobility and oil recovery factors. Therefore, alternating nanofluid and CO<sub>2</sub> flooding performs exceptionally well in low-permeability rock formations, a conclusion supported by wettability measurement results.

**Author Contributions:** J.H. and M.F. designed this experiment; J.H. and H.H. performed a series of experiments on the preparation of this thickener; M.L. performed fracturing fluid evaluation test experiments; J.H. and B.H. collated the experimental data; W.L. and L.C. were responsible for supervision. All authors have read and agreed to the published version of the manuscript.

**Funding:** This study was supported by the General Project of the National Natural Science Foundation of China “Research on mechanisms of high temperature thixotropy of thermosensitive polymer nanofluid” (No. 52074038).

**Informed Consent Statement:** Informed consent was obtained from all subjects involved in the study.

**Data Availability Statement:** The data presented in this study are available in the insert article.

**Conflicts of Interest:** The authors declare no conflict of interest.

## References

1. Kulkarni, M.M.; Rao, D.N. Experimental investigation of miscible and immiscible Water-Alternating-Gas (WAG) process performance. *J. Pet. Sci. Eng.* **2005**, *48*, 1–20. [[CrossRef](#)]
2. Muggeridge, A.; Cockin, A.; Webb, K.; Frampton, H.; Collins, I.; Moulds, T.; Salino, P. Recovery rates, enhanced oil recovery and technological limits. *Philosophical Transactions of the Royal Society A: Mathematical. Phys. Eng. Sci.* **2014**, *372*, 20120320.
3. Hu, W.R. Current status and future of low permeability oil and gas in China. *China Eng. Sci.* **2009**, *11*, 29–37.
4. Yang, X.; Zhao, W.; Zou, C.; Chen, M.; Guo, Y. Genetic mechanism of low-permeability reservoirs and formation and distribution of high-quality reservoirs. *Acta Pet. Sin.* **2007**, *4*, 57–61.
5. Hu, Z.; Ba, Z.; Xiong, W.; Gao, S.; Luo, R. Analysis of Micro Pore Structure of Low Permeability Reservoirs. *J. Daqing Pet. Inst.* **2006**, *3*, 51–53.
6. Wang, D.; Shi, D.; Li, X.; Chen, G. Analysis of the main contradiction mechanism and reasonable well spacing in the development of low-permeability sandstone reservoirs. *Pet. Explor. Dev.* **2003**, *1*, 87–89.

7. Ali, J.A.; Kolo, K.; Manshad, A.K.; Mohammadi, A.H. Recent advances in application of nanotechnology in chemical enhanced oil recovery: Effects of nanoparticles on wettability alteration, interfacial tension reduction, and flooding. *Egypt. J. Pet.* **2018**, *27*, 1371–1383. [[CrossRef](#)]
8. Li, B.; Zhang, D.; Lin, S.; Liu, F.; Li, Z. Indoor experimental study on frozen gel foam system. *Spec. Petrochem.* **2013**, *30*, 21–25.
9. Mahdavi, S.; James, L.A. High pressure and high-temperature study of CO<sub>2</sub> saturated-water injection for improving oil displacement; mechanistic and application study. *Fuel* **2020**, *262*, 116442. [[CrossRef](#)]
10. Aghdam, K.A.; Moghaddas, J.S.; Moradi, B.; Dabiri, M.; Hassanzadeh, M. Maximizing the oil recovery through miscible water alternating gas (WAG) injection in an Iranian oil reservoir. *Pet. Sci. Technol.* **2013**, *31*, 2431–2440. [[CrossRef](#)]
11. Wang, L.; Zhao, Q.; Li, Z. Experimental investigation of carbon dioxide flooding in heavy oil reservoirs for enhanced oil recovery. *Energy Rep.* **2022**, *8*, 10754–10761. [[CrossRef](#)]
12. Ghafoori, A.; Shahbazi, K.; Darabi, A.; Soleymanzadeh, A.; Abedini, A. The experimental investigation of nitrogen and carbon dioxide water-alternating-gas injection in a carbonate reservoir. *Pet. Sci. Technol.* **2012**, *30*, 1071–1081. [[CrossRef](#)]
13. Salehi, M.M.; Safarzadeh, M.A.; Sahraei, E.; Nejad, S.A. Comparison of oil removal in surfactant alternating gas with water alternating gas, water flooding and gas flooding in secondary oil recovery process. *J. Pet. Sci. Eng.* **2014**, *120*, 86–93. [[CrossRef](#)] [[PubMed](#)]
14. Cao, X.; Lu, G.; Wang, J.; Zhang, D.; Ren, M. Current Status and Future Research Directions of CO<sub>2</sub> Enhanced Oil Recovery Technology in Shengli Oilfield. *Reserv. Eval. Dev.* **2020**, *10*, 51–59.
15. Zhang, R.; Li, X.; Li, X.; Niu, M.; Li, R. Evaluation of CO<sub>2</sub> flooding effect and characteristics of reservoir damage in low-permeability heterogeneous multi-layer reservoirs. *Pet. Geol. Recovery Effic.* **2022**, *19*, 121–127.
16. Li, M.; Guan, H.; Hu, S.; Wang, X.; Li, Q.; Yuan, S. Parameter Optimization of CO<sub>2</sub> Huff-n-Puff and Non-Huff-n-Puff Water-Gas Alternating Injection in Ultra-Low Permeability Reservoirs. *Unconv. Oil Gas* **2021**, *8*, 60–66.
17. Zhang, M.; Zhao, F.; Lu, G.; Hou, J.; Song, L.; Feng, H.; Zhang, D. Adaptation Limits of Gas-Water Alternating to Improve CO<sub>2</sub> Enhanced Oil Recovery Effect. *Oilfield Chem.* **2020**, *37*, 279–286.
18. Lu, C.; Song, L.; Shang, F.; Yang, L.; Yang, R.; Guo, P.; Du, J. Study on Rational Displacement Method and Parameters Experiment of High-Temperature and High-Pressure Carbonate Reservoirs. *J. Shaanxi Univ. Sci. Technol.* **2022**, *40*, 96–101.
19. Christensen, J.; Stenby, E.; Skauge, A. Review of WAG field experience. *SPE Reserv. Eval. Eng.* **2001**, *4*, 97–106. [[CrossRef](#)]
20. Zhang, J.; Zhang, H.; Ma, L.; Liu, Y.; Zhang, L. Performance evaluation and mechanism with different CO<sub>2</sub> flooding modes in tight oil reservoir with fractures. *J. Pet. Sci. Eng.* **2020**, *188*, 106950. [[CrossRef](#)]
21. Chaturvedi, K.R.; Ravilla, D.; Kaleem, W.; Jadhawar, P.; Sharma, T. Impact of low salinity water injection on CO<sub>2</sub> storage and oil recovery for improved CO<sub>2</sub> utilization. *Chem. Eng. Sci.* **2021**, *229*, 116127. [[CrossRef](#)]
22. Ding, S.; Wang, L.; Li, M.; Zhang, W.; Liu, H.; Sun, J. Study on Control Technology of Carbon Dioxide Flooding Gas Channeling in Low Permeability Reservoir. In Proceedings of the International Field Exploration and Development Conference; Springer: Singapore, 2021; pp. 2786–2794.
23. Rezk, M.; Allam, N. Impact of nanotechnology on enhanced oil recovery: A mini-review. *Ind. Eng. Chem. Res.* **2019**, *58*, 16287–16295. [[CrossRef](#)]
24. Crews, J.; Huang, T. Performance enhancements of viscoelastic surfactant stimulation fluids with nanoparticles. In Proceedings of the Europec/EAGE Conference and Exhibition, SPE, Rome, Italy, 9–12 June 2008; p. 113533.
25. Kanj, M.; Funk, J.; Al-Yousif, Z. Nanofluid coreflood experiments in the ARAB-D. In Proceedings of the SPE Saudi Arabia Section Technical Symposium, SPE, Al-Khobar, Saudi Arabia, 9–11 May 2009; p. 126161.
26. Lan, Q.; Yang, F.; Zhang, S.; Liu, S.; Xu, J.; Sun, D. Synergistic effect of silica nanoparticle and cetyltrimethyl ammonium bromide on the stabilization of O/W emulsions. *Colloids Surf. A* **2007**, *302*, 126–135. [[CrossRef](#)]
27. Li, S.; Dan, D.; Lau, H.; Hadia, N.; Torsæter, O.; Stubbs, L. Investigation of wettability alteration by silica nanoparticles through advanced surface-wetting visualization techniques. In Proceedings of the SPE Annual Technical Conference and Exhibition, SPE, Calgary, AB, Canada, 30 September–2 October 2019; p. D031S040R002.
28. Yuan, W.; Liu, X.; Wei, H.; Liu, J.; Yang, H.; Hu, S.; Li, Y.; Wang, D. Research and application effect of polymeric microsphere in Wen-10 of Sinopec Zhongyuan Oil field. *Inner Mong. Petrochem* **2010**, *12*, 122–126.
29. Li, X.; Ying, Z.; Jia, Y.; Liu, X.; Yang, T.; Ma, L. Application of nanosphere deep profile control and displacement technology in Changqing oilfield. *Oilfield Chem* **2012**, *29*, 419–422.
30. Tian, Q.; Wang, L.; Tang, Y.; Liu, C.; Ma, C.; Wang, T. Research and Application of Nano Polymer Microspheres Diversion Technique of Deep Fluid. In Proceedings of the SPE International Oilfield Nanotechnology Conference and Exhibition, SPE, Noordwijk, The Netherlands, 12–14 June 2012; p. 156999.
31. Al-Shargabi, M.; Davoodi, S.; Wood, D.; Al-Musai, A.; Rukavishnikov, V.; Minaev, K. Nanoparticle applications as beneficial oil and gas drilling fluid additives: A review. *J. Mol. Liq.* **2022**, *352*, 118725. [[CrossRef](#)]
32. Ershadi, M.; Alaei, M.; Rashidi, A.; Ramazani, A.; Khosravani, S. Carbonate and sandstone reservoirs wettability improvement without using surfactants for Chemical Enhanced Oil Recovery. *Fuel* **2015**, *153*, 408–415. [[CrossRef](#)]
33. Lau, H.; Yu, M.; Nguyen, Q. Nanotechnology for oilfield applications: Challenges and impact. *J. Pet. Sci. Eng.* **2017**, *157*, 1160–1169. [[CrossRef](#)]
34. Singh, S.; Ahmed, R. Vital role of nanopolymers in drilling and stimulations fluid applications. In Proceedings of the SPE Annual Technical Conference and Exhibition, SPE, Florence, Italy, 19–22 September 2010; p. 130413.

35. Aziz, H.; Muther, T.; Khan, M.; Syed, F. A review on nanofluid water alternating gas (N-WAG): Application, preparation, mechanism, and challenges. *Arab. J. Geosci.* **2021**, *14*, 1416. [[CrossRef](#)]
36. Chen, B.; Reynolds, A.C. Ensemble-based optimization of the water-alternating-gas-injection process. *SPE J.* **2016**, *21*, 0786–0798. [[CrossRef](#)]
37. Cheraghian, G. A new thermal method concept for IOR from oil reservoir using optimized in-situ combustion. In Proceedings of the 78th EAGE Conference and Exhibition, Online, 30 May–2 June 2016; pp. 1–3.
38. Cheraghian, G.; Tardasti, S. Improved Oil Recovery by the Efficiency of Nano-particle in Imbibition Mechanism. In Proceedings of the 2nd EAGE International Conference KazGeo, Almaty, Kazakhstan, 29–31 October 2012; European Association of Geoscientists & Engineers: Utrecht, The Netherlands, 2012; p. 315.
39. Ju, B.; Fan, T.; Ma, M. Enhanced oil recovery by flooding with hydrophilic nanoparticles. *China Particul.* **2006**, *4*, 41–46. [[CrossRef](#)]
40. Cheraghian, G.; Nezhad, S.; Kamari, M.; Hemmati, M.; Masihi, M.; Bazgir, S. Effect of nanoclay on improved rheology properties of polyacrylamide solutions used in enhanced oil recovery. *J. Pet. Explor. Prod. Technol.* **2014**, *5*, 189–196. [[CrossRef](#)]
41. Cheraghian, G.; Nezhad, S.S.K.; Kamari, M.; Hemmati, M.; Masihi, M.; Bazgir, S. Adsorption polymer on reservoir rock and role of the nanoparticles, clay and SiO<sub>2</sub>. *Int. Nano Lett.* **2014**, *4*, 114. [[CrossRef](#)]
42. Le, N.; Pham, D.; Le, K.; Nguyen, P. Design and screening of synergistic blends of SiO<sub>2</sub> nanoparticles and surfactants for enhanced oil recovery in high-temperature reservoirs. *Adv. Nat. Sci. Nanotechnol.* **2011**, *2*, 35013–35019. [[CrossRef](#)]
43. Raj, L.; Qu, M.; Xiao, L.; Hou, J.; Li, Y.; Liang, T.; Zhao, M. Ultralow concentration of molybdenum disulfide nanosheets for enhanced oil recovery. *Fuel* **2019**, *251*, 514–522. [[CrossRef](#)]
44. Eltoun, H.; Yang, Y.; Hou, J. The effect of nanoparticles on reservoir wettability alteration: A critical review. *Pet. Sci.* **2021**, *18*, 136–153. [[CrossRef](#)]
45. Alomair, O.; Matar, K.; Alsaheed, Y. Experimental study of enhanced-heavy-oil recovery in Berea sandstone cores by use of nanofluids applications. *SPE Reserv. Eval. Eng.* **2015**, *18*, 387–399. [[CrossRef](#)]
46. Rezvani, H.; Khalilnezhad, A.; Ganji, P.; Kazemzadeh, Y. How ZrO<sub>2</sub> nanoparticles improve the oil recovery by affecting the interfacial phenomena in the reservoir conditions. *J. Mol. Liq.* **2018**, *252*, 158–168. [[CrossRef](#)]
47. Mohajeri, M.; Hemmati, M.; Shekarabi, A. An experimental study on using a nanosurfactant in an EOR process of heavy oil in a fractured micromodel. *J. Pet. Sci. Eng.* **2015**, *126*, 162–173. [[CrossRef](#)]
48. Wang, Z.; Babadagli, T.; Maeda, N. Preliminary screening and formulation of new generation nanoparticles for stable pickering emulsion in cold and hot heavy-oil recovery. *SPE Reserv. Eval. Eng.* **2021**, *24*, 66–79. [[CrossRef](#)]
49. Qi, L.; Song, C.; Wang, T.; Li, Q.; Hirasaki, G.; Verduzco, R. Polymer-coated nanoparticles for reversible emulsification and recovery of heavy oil. *Langmuir* **2018**, *34*, 6522–6528. [[CrossRef](#)] [[PubMed](#)]
50. Lei, Q.; Luo, J.; Peng, B.; Wang, X.; Xiao, P.; Wang, P.; Geng, X. Mechanism of expanding swept volume by nano-sized oil-displacement agent. *Pet. Explor. Dev.* **2019**, *46*, 991–997. [[CrossRef](#)]
51. Jin, Y.; Wang, Z.; Sun, Q.; Li, Y.; Wang, B.; Chen, Y. Research and application of nano-injection technology for tight reservoirs. *Spec. Oil Gas Reserv.* **2023**, *30*, 169–174.
52. Moslan, M.; Wan Sulaiman, W.; Ismail, A.; Jaafar, M.; Ismail, I. Wettability alteration of dolomite rock using nanofluids for enhanced oil recovery. *Mater. Sci. Forum* **2016**, *864*, 194–198. [[CrossRef](#)]
53. Nourafkan, E.; Hu, Z.; Wen, D. Nanoparticle-enabled delivery of surfactants in porous media. *J. Colloid Interface Sci.* **2018**, *519*, 44–57. [[CrossRef](#)]
54. Ju, B.; Fan, T. Experimental study and mathematical model of nanoparticle transport in porous media. *Powder Technol.* **2009**, *192*, 195–202. [[CrossRef](#)]
55. Li, S.; Torsaeter, O. The impact of nanoparticles adsorption and transport on wettability alteration of intermediate wet berea sandstone. In Proceedings of the SPE Middle East Unconventional Resources Conference and Exhibition, Muscat, Oman, 26–28 January 2015. Society of Petroleum Engineers.
56. Ogolo, N.A.; Olafuyi, O.A.; Onyekonwu, M.O. Enhanced Oil Recovery Using Nanoparticles. In Proceedings of the SPE Saudi Arabia Section Technical Symposium and Exhibition, Al-Khobar, Saudi Arabia, 8–11 April 2012; pp. 12–18.
57. Al Matroushi, M.; Pourafshary, P.; Al Wahaibi, Y. Possibility of nanofluid/gas alternating injection as an EOR method in an oil field. In Proceedings of the Abu Dhabi International Petroleum Exhibition and Conference, SPE, Abu Dhabi, UAE, 9–12 November 2015; p. D031S054R002.
58. Salem Ragab, A.; Hannora, A. Comparative investigation of nano particle effects for improved oil recovery—experimental work. In Proceedings of the SPE Kuwait Oil and Gas Show and Conference, SPE, Mishref, Kuwait, 11–14 October 2015.
59. Wang, K.; Liang, S.; Wang, C. Research of improving water injection effect by using active SiO<sub>2</sub> nano-powder in the low-permeability oilfield. *Adv. Mater. Res.* **2010**, *92*, 207–212. [[CrossRef](#)]
60. Amrouche, F.; Gomari, S.; Islam, M.; Xu, D. A novel hybrid technique to enhance oil production from oil-wet carbonate reservoirs by combining a magnetic field with alumina and iron oxide nanoparticles. *J. Clean. Prod.* **2021**, *281*, 124891. [[CrossRef](#)]
61. Gallo, G.; Erdmann, E. Simulation of viscosity enhanced CO<sub>2</sub> nanofluid alternating gas in light oil reservoirs. In Proceedings of the SPE Latin America and Caribbean Petroleum Engineering Conference, SPE, Buenos Aires, Argentina, 17–19 May 2017.
62. Ragab, A.M.; Hannora, A.E. An experimental investigation of silica nano particles for enhanced oil recovery applications. In Proceedings of the SPE North Africa Technical Conference and Exhibition, SPE, Cairo, Egypt, 14–15 September 2015; p. 175829.

63. Mo, D.; Jia, B.; Yu, J.; Liu, N.; Lee, R. Study nanoparticle-stabilized CO<sub>2</sub> foam for oil recovery at different pressure, temperature, and rock samples. In Proceedings of the SPE Improved Oil Recovery Symposium, SPE, Tulsa, OK, USA, 12–16 April 2014; p. 169110.
64. Lee, J.; Huang, J.; Babadagli, T. Visual support for heavy-oil emulsification and its stability for cold-production using chemical and nano-particles. In Proceedings of the SPE Annual Technical Conference and Exhibition, SPE, Calgary, AB, Canada, 30 September–2 October 2019; p. 196023.
65. Lee, J.; Babadagli, T. Optimal design of pickering emulsions for heavy-oil recovery improvement. *J. Dispers. Sci. Technol.* **2020**, *41*, 2048–2062. [[CrossRef](#)]

**Disclaimer/Publisher’s Note:** The statements, opinions and data contained in all publications are solely those of the individual author(s) and contributor(s) and not of MDPI and/or the editor(s). MDPI and/or the editor(s) disclaim responsibility for any injury to people or property resulting from any ideas, methods, instructions or products referred to in the content.